ARTICLE

Hypomorphic Recessive Variants in *SUFU* Impair the Sonic Hedgehog Pathway and Cause Joubert Syndrome with Cranio-facial and Skeletal Defects

Roberta De Mori,[1,2,20] Marta Romani,[3,20] Stefano D'Arrigo,[4] Maha S. Zaki,[5] Elisa Lorefice,[1] Silvia Tardivo,[1] Tommaso Biagini,[6] Valentina Stanley,[7] Damir Musaev,[7] Joel Fluss,[8] Alessia Micalizzi,[1,2] Sara Nuovo,[1,9] Barbara Illi,[10] Luisa Chiapparini,[11] Lucia Di Marcotullio,[12] Mahmoud Y. Issa,[5] Danila Anello,[1] Antonella Casella,[1] Monia Ginevrino,[1,13] Autumn Sa'na Leggins,[7] Susanne Roosing,[14] Romina Alfonsi,[12] Jessica Rosati,[15] Rachel Schot,[16] Grazia Maria Simonetta Mancini,[16] Enrico Bertini,[17] William B. Dobyns,[18,19] Tommaso Mazza,[6] Joseph G. Gleeson,[7] and Enza Maria Valente[1,13,*]

The Sonic Hedgehog (SHH) pathway is a key signaling pathway orchestrating embryonic development, mainly of the CNS and limbs. In vertebrates, SHH signaling is mediated by the primary cilium, and genetic defects affecting either SHH pathway members or ciliary proteins cause a spectrum of developmental disorders. SUFU is the main negative regulator of the SHH pathway and is essential during development. Indeed, *Sufu* knock-out is lethal in mice, and recessive pathogenic variants of this gene have never been reported in humans. Through whole-exome sequencing in subjects with Joubert syndrome, we identified four children from two unrelated families carrying homozygous missense variants in *SUFU*. The children presented congenital ataxia and cerebellar vermis hypoplasia with elongated superior cerebellar peduncles (mild "molar tooth sign"), typical cranio-facial dysmorphisms (hypertelorism, depressed nasal bridge, frontal bossing), and postaxial polydactyly. Two siblings also showed polymicrogyria. Molecular dynamics simulation predicted random movements of the mutated residues, with loss of the native enveloping movement of the binding site around its ligand GLI3. Functional studies on cellular models and fibroblasts showed that both variants significantly reduced SUFU stability and its capacity to bind GLI3 and promote its cleavage into the repressor form GLI3R. In turn, this impaired SUFU-mediated repression of the SHH pathway, as shown by altered expression levels of several target genes. We demonstrate that germline hypomorphic variants of *SUFU* cause deregulation of SHH signaling, resulting in recessive developmental defects of the CNS and limbs which share features with both SHH-related disorders and ciliopathies.

Introduction

Embryonic development is a highly complex process that is tightly regulated by evolutionary conserved signaling pathways. Among these, the Sonic Hedgehog (SHH) pathway plays a central role in controlling cell patterning and differentiation of several embryonic structures, such as the central nervous system (CNS) and the limbs. In the developing CNS, SHH is secreted by the notochord and floor plate and forms a ventral to dorsal gradient that regulates diverse essential processes such as specification of ventral fate, proliferation, and axonal guidance.[1,2] Similarly, SHH orchestrates several aspects of cerebellar development, initially stimulating the proliferation of cerebellar progenitors in the rhombic lip and the ventricular zone, and later that of granule cell precursors in the external granular layer.[3,4] During formation of the limb skeleton, SHH is required for the survival and expansion of distal chondrogenic progenitor cells and for specification of digit identities along the anterior-posterior axis.[5]

In vertebrates, SHH signaling is critically mediated by the primary cilium, a microtubule-based organelle protruding from the surface of nearly all cell types. Many components of the SHH pathway are variably localized within the cilia at different steps of pathway activation,[6,7] and the malfunctioning of many ciliary genes is known to impair SHH signaling.[8–11] When the pathway is inactive, the SHH receptor PTCH1 inhibits the ciliary

---

CrossMark

localization and activation of the seven-pass membrane protein SMO. In this condition, the effectors GLI2 and GLI3 are restrained to the cytoplasm, where they form a complex with Suppressor of Fused (SUFU), the main negative regulator of the pathway, and undergo partial proteasomal-mediated proteolysis. This removes the C terminus activation domain and generates the transcriptional repressor forms GLI3R and, to a lesser extent, GLI2R. Upon SHH binding, PTCH1 exits the cilium relieving SMO inhibition. This promotes the progressive dissociation of SUFU from GLI2-3 proteins, their translocation to the cilium tip, and inhibition of their cleavage, leading to the formation of the transcriptional activators GLI2A and GLI3A. In turn, these translocate to the nucleus to activate the expression of several target genes, such as *GLI1* (MIM: 165220), *BCL2* (MIM: 151430), and *PTCH1* itself (MIM: 601309).[12–14] As GLI1 lacks the N-terminal repression domain, it works exclusively as a transcriptional activator whose activity is also constrained by SUFU, and appears to function as part of a positive feedback loop to reinforce the transcriptional output of SHH signaling.[15]

Ciliopathies such as Joubert syndrome (JS [MIM: 213300]), acrocallosal syndrome (ACLS [MIM: 200990]), and oral-facial-digital syndromes (MIM: 311200, 277170) frequently present with congenital defects of the CNS (e.g., cerebellar vermis hypoplasia, "molar tooth sign" [MTS], defects of the corpus callosum, polymicrogyria), midline facial anomalies, and polydactyly, which are at least partially attributed to altered SHH signaling.[16–19] Similarly, heterozygous pathogenic variants directly affecting several members of the SHH pathway, including *SHH* itself (MIM: 600725), *PTCH1*, *SMO* (MIM: 601500), *GLI2* (MIM: 165230), or *GLI3* (MIM: 165240), result in a spectrum of autosomal-dominant developmental disorders including holoprosencephaly (MIM: 142945), schizencephaly with polymicrogyria (MIM: 269160), Curry-Jones syndrome (CJS [MIM: 601707]), Greig cephalopolysyndactyly syndrome (GCPS [MIM: 175700]), Pallister-Hall syndrome (MIM: 146510), and non-syndromic polydactylies (MIM: 174200, 174700), that are variably characterized by anomalies of the brain, midline face, and/or limbs.[20–23]

An aberrant activity of the SHH pathway has also been firmly associated with increased risk of developing cancer. Germline heterozygous loss-of-function variants of either *PTCH1* or *SUFU* (MIM: 607035) may cause a complex condition termed nevoid-basal-cell carcinoma syndrome (Gorlin syndrome [MIM: 109400]), characterized by the occurrence of several basal cell carcinomas and other cancers at a young age (<20 years), variably associated with developmental and skeletal abnormalities.[24,25] Moreover, somatic variants of *PTCH1* or *SMO*, and both germinal and somatic variants of *SUFU*, have been found to predispose to a variety of tumors, such as basal cell carcinoma, meningioma, and cerebellar medulloblastoma (MIM: 605462, 607174, 155255).[26–30]

To date, germline recessive pathogenic variants of *SUFU* have never been reported in human subjects, supporting the essential role of SUFU in embryonic development. *Sufu* knock-out mice display early embryonic lethality at E9.5, with severe cranio-facial and neural closure defects related to constitutive SHH pathway activation,[31] similar to that observed in *Ptch1* mutants.[32] Limb-specific conditional deletion of *Sufu* results in polydactyly due to a block in Gli3R processing,[33,34] whereas mouse embryos with conditional knock-out of *Sufu* in the mid-hindbrain show altered morphology of the brainstem and cerebellum and delayed differentiation and abnormal migration of most cerebellar cell types.[35]

Here, we show that germline hypomorphic variants of *SUFU* cause deregulation of the SHH pathway, resulting in recessive stereotypical developmental defects of the CNS and limbs which share peculiar features with both SHH-related disorders and with ciliopathies such as JS.

Subjects, Material, and Methods

Subjects

Two large cohorts of subjects with neuroradiologically confirmed JS or related cerebellar and brainstem defects have been recruited at the IRCCS Santa Lucia Foundation (Rome, Italy) and the University of California San Diego (La Jolla, CA, United States). After obtaining written informed consent from the affected subjects, parents, or legal representatives, detailed clinical data and brain MRI scans were obtained from the referring clinicians. Ethics approval has been obtained by the local Ethics Committees.

A cohort of 60 subjects with polymicrogyria (mostly familial), negative for pathogenic variants in known genes, was recruited through international collaborations.

Sequencing and Data Analysis

As part of ongoing research projects to identify the genetic causes of brain ciliopathies and related conditions, 385 probands underwent whole-exome sequencing (WES) and data were filtered as previously described.[36,37] Subjects found to carry pathogenic variants in known genes associated to ciliopathies or other congenital defects were excluded from further studies. Pathogenicity and conservation of identified variants were predicted using several commonly used software (Table S1).

Bidirectional Sanger sequencing of the 12 exons and exon-intron junctions of *SUFU* was performed using the Big Dye Terminator chemistry (Applied Biosystems) in 60 probands with polymicrogyria (mostly familial) and 100 healthy Italian control subjects. Moreover, *SUFU* was included in a panel of 120 known and candidate ciliopathy genes, for next generation sequencing-based targeted sequencing in a distinct cohort of 346 probands with JS or related ciliopathies. Targeted resequencing was performed on a Solid 5500xL platform using the TargetSeq Custom Enrichment System (ThermoFisher Scientific), as previously reported.[36]

In Silico Modeling of *SUFU* Missense Variants

Atomic coordinates of SUFU, in complex with GLI3, were obtained from the Protein Data Bank[38] (PDB: 4BLD) and used for Molecular Dynamics (MD) simulations. The residues of the considered PDB file correspond to residues 28–285 and 345–480 of SUFU and residues 333–340 of GLI3. The wild-type (WT) model was mutated *in silico* to introduce p.Ile406Thr and p.His176Arg variants through UCSC Chimera,[39] yielding two further models. All three models were embedded in boxes, extending up to 12 Å, and solvated using the TIP3P water model. The tleap tool was also used to add counter ions in order to neutralize the overall charge of the models. Each of them was first energy-minimized and then equilibrated for approximately 5 ns, by time steps of 1 fs. MD simulations were performed three times on the three equilibrated models for 200 ns by time steps of 2 fs, namely for 100 million steps. A 10 Å cutoff was used for non-bonded short-range interactions, and long-range electrostatics were treated with the particle-mesh Ewald method. Temperature and pressure were maintained at 300 K and 101.3 kPa, respectively, using the Langevin dynamics and piston method.

To analyze whether the protein was stable and close to the experimental structure, the following measures were calculated in WT and mutant proteins: (1) root-mean-square deviation (RMSD), that measures the average distance between all heavy atoms (in this case C_α atomic coordinates) with respect to the X-ray structure; (2) root mean square fluctuation (RMSF), measuring the deviation over time between the positions of the C_α atomic coordinates of each residue with respect to the X-ray structure; and (3) dynamic cross correlation maps (DCCMs), that allow investigation of the long-range interactions of atoms. Peaks, corresponding to the C_{ij} elements of the map, are indicative of strong to moderate positive correlation (red to green) or of strong to moderate anti-correlation (dark to light blue) between residues *i-j*. Per-residue RMSF, hydrogen bonds, and secondary structure content were determined with the Gromacs tools: *g_rmsf*, *g_hbond* and *do_dssp*. 3D figures and motions were generated with UCSC Chimera.

Cell Cultures and Treatments

Skin-derived primary fibroblasts from the two probands (COR369 II:1 and MTI-2023 II:2, Figure S1) and from two healthy control subjects were cultured in Dulbecco's Modified Eagle Medium (DMEM) supplemented with inactivated 20% fetal bovine serum (FBS), 2 mM L-glutamine, and 1% penicillin/streptomycin, at 5% CO_2 and 37°C. Medium was replaced once a week until fibroblasts expanded. Fibroblasts were detached with trypsin (EuroClone) and replated for at least two passages. The day before treatments, 3×10^5 fibroblasts were plated in a 60 mm dish. IMCD3 cells were grown in DMEM F12, supplemented with inactivated 10% FBS, 2 mM L-glutamine, and 1% penicillin/streptomycin, at 5% CO_2 and 37°C.

Before treatments, cells were starved in DMEM with 0.1% FBS, 2 mM L-glutamine, and 1% penicillin/streptomycin. Treatments were: 40 μM cycloheximide (Sigma-Aldrich) for 24 hr, 50 μM MG132 (Sigma-Aldrich) for 6 hr, and 200 nM Smoothened Agonist (SAG) (Adipogen) for 12 hr.

Expression Vectors and Transfection

The QuikChange II Site-Directed Mutagenesis kit (Applied Biosystem) was used to insert either the p.Ile406Thr or the p.His176Arg change in pSufu WT vector,[40] according to the manufacturer's instructions. Constructs were transformed by heat shock into DH5α competent bacteria, grown in LB at 37°C overnight and purified using the EndoFree Plasmid Maxi kit (QIAGEN). Plasmids were quantified by Nanodrop (ThermoFisher Scientific) and verified by Sanger sequencing following standard protocol. Transfection experiments were performed using Lipofectamine 2000 (Invitrogen) as recommended by the supplier.

Cilia Formation and Immunofluorescence

Fibroblasts were plated onto coverslips and cultured in DMEM with 20% FBS until 80% confluence. Thereafter, they were serum starved for 24 hr in DMEM 0.1% FBS to allow cilia formation. Cells were fixed in cold methanol and coverslips were rinsed and blocked in PBS with 10% BSA prior to incubation with antibodies. For immunofluorescence, we used acetylated-α-tubulin, γ-tubulin, HA or FLAG primary antibodies (Sigma-Aldrich) overnight followed by incubation with goat anti-mouse Alexa Fluor 555 and goat anti-rabbit Alexa Fluor 488. Nuclei were stained with Hoechst (Invitrogen). Images were analyzed at a confocal microscope (C2 Confocal Microscopy System), either at 488 nm (green) or 561 nm (red), by using a 60× 1.4 NA Plan Apo objective (Nikon Corporation) and captured by NIS Element AR 4.13.04 software.

Cell Extracts and Western Blot

Cells were lysed in RIPA buffer. Protein amount was determined by Bradford protein assay kit (BioRad). Lysates were boiled for 5 min after dithiothreitol (DTT 200 mM, Sigma-Aldrich) addition. Proteins were loaded on SDS-polyacrylamide gels and transferred to nitrocellulose by standard procedures.

Antibodies were used against the following proteins or peptides: SUFU (Cell Signaling), GAPDH and HA (Sigma-Aldrich), GLI3 and GLI1 (R&D). All the antibodies were used according to the manufacturer's instructions. Densitometric analyses were performed with the ImageQuant software.

Co-immunoprecipitation

Transfected IMCD3 cells were lysed in RIPA 1× buffer containing 1% protease inhibitor and 1% phosphatase inhibitor (ThermoFisher Scientific) and 500 μg of total lysate
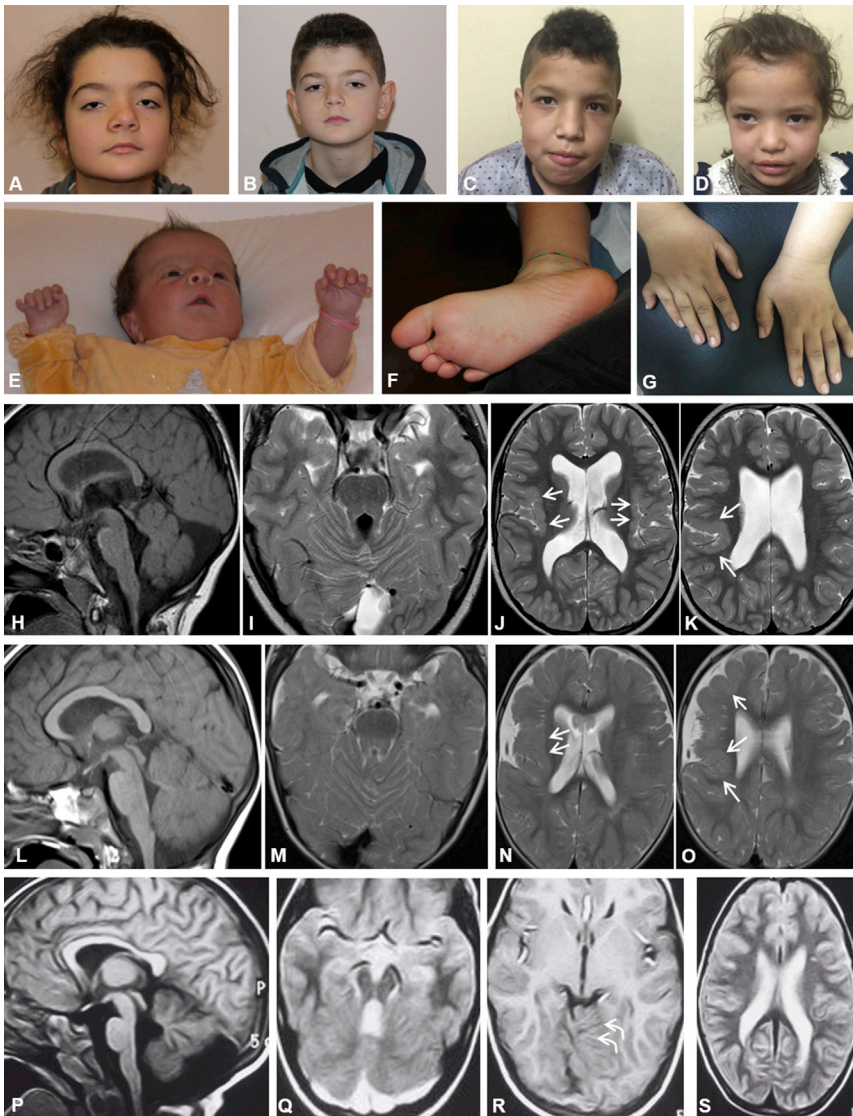
Figure 1. Clinical and Neuroimaging Features of Subjects Harboring *SUFU* Homozygous Missense Variants

(A–D) Photographs of the four children from families COR369 (A, B) and MTI-2023 (C, D). Note hypertelorism, frontal bossing, and broad, depressed nasal bridge.

(E and F) Bilateral hand post-axial polydactyly (E) and plantar dyskeratotic pits (F) in the male sibling from family COR369.

(G) Right hand post-axial polydactyly in the male sibling from family MTI-2023.

(H–O) Brain MRI of affected girl (H–K) and boy (L–O) from family COR369. Note mild vermis hypoplasia (H, L) and elongated, thickened, and horizontally orientated superior cerebellar peduncles consistent with mild MTS (I, M), associated with bilateral polymicrogyria mainly involving the right perisylvian regions (arrows in J, K, N, O). Also note the megacisterna magna in the sagittal image of the girl (H).

(P–S) Brain MRI in the proband from family MTI-2023. Note vermis hypoplasia, megacisterna magna (P, Q), dysplastic foliar abnormalities (curved arrows in R), deep interpeduncular fossa, and thickened horizontally orientated superior cerebellar peduncles (mild MTS, Q).

In all subjects, mild lateral ventricular enlargement and shrunken white matter in the supratentorial posterior regions are visible (K, N, O, S). MRI of the fourth child were not available for publication.

were used for immunoprecipitation. The lysate was incubated with beads, directly conjugated with HA antibody (Red anti-HA beads, Sigma-Aldrich), overnight at 4°C. The day after, the immunocomplexes were washed three times in lysis buffer, resuspended in 25 μL of sample buffer, and finally processed in western blotting (WB).

Real-Time Quantitative PCR

Total RNA was extracted from fibroblasts with the High Pure RNA Isolation Kit (Roche). A total amount of 500 ng RNA was reverse transcribed using the High Capacity cDNA Reverse Transcription Kit (Applied Biosystems), according to the manufacturer's instructions. After cDNA synthesis, samples were loaded in duplicate into a 384-well Custom TaqMan Array Card (ThermoFisher Scientific) and run on an ABI Prism 7900HT sequence detection system (Applied Biosystems). This whole experiment was run in triplicate. β-actin was used as internal control to normalize the data on each card, as well as between cards.

Statistical Analysis

qRT-PCR data are expressed as mean ± standard error (SE). Data analyses and statistical evaluations were performed using the computing environment R (v.3.4.0). A two-tailed Student's t test was applied to identify genes that were differentially expressed between two groups and a value of $p < 0.05$ was deemed statistically significant.

Results

Identification of *SUFU* Recessive Missense Variants

In our combined cohorts of subjects with JS and related disorders, we identified four children from two unrelated families (COR369 from Italy and MTI-2023 from Egypt) with similar clinical presentation, who carried homozygous missense variants of *SUFU* (Figure S1). All subjects presented peculiar facial dysmorphisms (hypertelorism, broad and depressed nasal bridge, frontal bossing), oculomotor apraxia, developmental delay with mild intellectual impairment, gait ataxia, and dysarthria. Three of them had post-axial polydactyly and two had global macrosomia with macrocephaly. One child also showed a few small dyskeratotic pits on the foot soles (Figures 1A–1G). There were no other signs of systemic involvement, except for mild

retinopathy in one sibling from family COR369. Brain imaging showed cerebellar vermis hypoplasia with elongated superior cerebellar peduncles and deepened interpeduncular fossa (mild MTS) in all children; in addition, the two siblings from family COR369 had bilateral polymicrogyria mainly involving the perisylvian regions (Figures 1H–1S). A detailed description of the four affected children is provided in Supplemental Note and Table S2.

In family COR369, two distinct homozygous missense variants survived the steps of stringent filtering of WES data, Sanger validation, and segregation analysis: hg19:10: g.104377106T>C; c.1217T>C (p.Ile406Thr) in *SUFU* (GenBank: NM_016169.3) and hg19:10: g.85973943A>T; c.2146A>T (p.Thr716Ser) in *CDHR1* (MIM: 609502; GenBank: NM_033100) (Figure S2). Both variants are absent from all public databases (dbSNP, EVS, gnomAD, Human Longevity Database) and from in-house WES databases consisting of more than 6,000 samples and are unanimously predicted to be deleterious (Table S1). Only one individual in the gnomAD database carried a heterozygous missense variant affecting the same SUFU residue but resulting in a different amino acid change (c.1218C>G [p.Ile406Met]). *CDHR1* (also termed *PCDH21*) is expressed only in the outer nuclear layer of the retina and encodes for protocadherin 21. Recessive variants of this gene are known to cause a form of cone-rod dystrophy with onset in the late second decade of life (MIM: 613660).

In family MTI-2023, only the hg38:10: g.102592654A>G; c.527A>G (p.His176Arg) variant in *SUFU* survived bioinformatic filtering of WES data and segregation analysis (Figure S2). This variant is absent from public databases and our in-house dataset, which includes sequencing data from more than 3,000 Egyptian individuals, and is predicted to have a deleterious impact on the protein function (Table S1).

An additional 12/731 (1.6%) probands carried heterozygous rare variants of *SUFU* (Table S3), while no pathogenic variants were detected in 60 subjects with isolated polymicrogyria or in 100 Italian control subjects.

Dynamic Properties of Mutant SUFU Proteins

The SUFU protein alternates between "open" and "closed" conformations. The closed form is stabilized by the binding with GLI proteins, whereas the open state is caused by the dissociation from GLI. Changes of critical residues on the interface between SUFU and GLI proteins may disrupt their complex and prevent SUFU from repressing GLI-mediated transcription. To assess the pathogenic effect of the identified missense variants, we first investigated their structural and dynamic impact on the SUFU protein (Figure 2A) by means of a series of molecular dynamics tools.

SUFU WT reached a stable state already after 60 ns of simulation, recording an RMSD of ~0.3 nm. Conversely, both SUFU mutants exhibited RMSD levels around 0.5 nm, after a longer stabilization stage of 150 ns (Figure 2B). Moreover, mutants turned out to be more flexible than WT. The loop made by the amino acid residues 354–385 was the most fluctuating region in all models but reached very high values (1.4 nm) for SUFU[p.Ile406Thr]. SUFU[p.His176Arg] also showed altered RMSF values compared to WT, mainly affecting the region nearby the mutation, which is known to participate in the formation of the GLI3-binding pocket (Figure 2C).

DCCMs of both mutants versus WT showed a dramatic change in the protein dynamics. In the WT model, the linker domain moved in a highly anti-correlated way with both the C-terminal and the N-terminal regions of the core domain. The SUFU[p.Ile406Thr] mutant acquired intra-domain anti-correlated motions in the C-terminal domain and in the N-terminal domain but completely changed the inter-domain correlated and anti-correlated motions. SUFU[p.His176Arg] exhibited a similar trend about the C-terminal domain, but it lost any motion between residues in the N-terminal domain. Overall, both mutants displayed random movements of the residues within the C-terminal domain and loss of the native enveloping movement of the binding site around GLI3 protein (Figure 2D, Movie S1).

To confirm the observed major perturbation of SUFU-GLI3 complex activity, we analyzed the modification of hydrogen bonds (h-bonds) between residues that constitute the SUFU-GLI3 binding site, as well as the size of the binding pocket. The GLI3 peptide, indeed, fits snugly into a narrow channel with the histidine from the SYGH motif, protruding into a binding pocket where it forms hydrogen-bonding interactions with specific amino acids.[41] During 200 ns simulation time, the WT protein repeatedly changed the size of the binding site and the number of h-bonds depending on the alternative open or closed conformations, while both mutants kept an almost stable distance between amino acids constituting the binding site and an almost constant number of h-bonds with GLI3 (Figures 2E and 2F). Overall, these findings suggest that both mutants hamper significantly the functional open/close states of the protein to different extents.

SUFU Missense Variants Reduce Protein Stability

It is well established that activation of the SHH pathway in mammals is mediated by primary cilia, and that pathogenic variants in *KIF7*, which is a key inhibitor of the pathway, cause a spectrum of phenotypes overlapping with the typical features of JS.[19,42] We then tested whether the identified *SUFU* missense variants could affect ciliogenesis but did not observe any abnormality in ciliary length or morphology in starved mutant fibroblasts compared to controls (Figure S3).

To evaluate whether *SUFU* variants could impact protein stability, IMCD3 cells were transfected with HA-tagged SUFU WT, SUFU[p.Ile406Thr], or SUFU[p.His176Arg] for 24, 48, and 72 hr and processed by WB. Mutant SUFU protein levels were significantly lower than WT already at 24 hr and decreased rapidly, with SUFU[p.Ile406Thr] almost disappearing at 72 hr after transfection (Figure 3A). Moreover, confocal microscopy analysis showed an abnormal
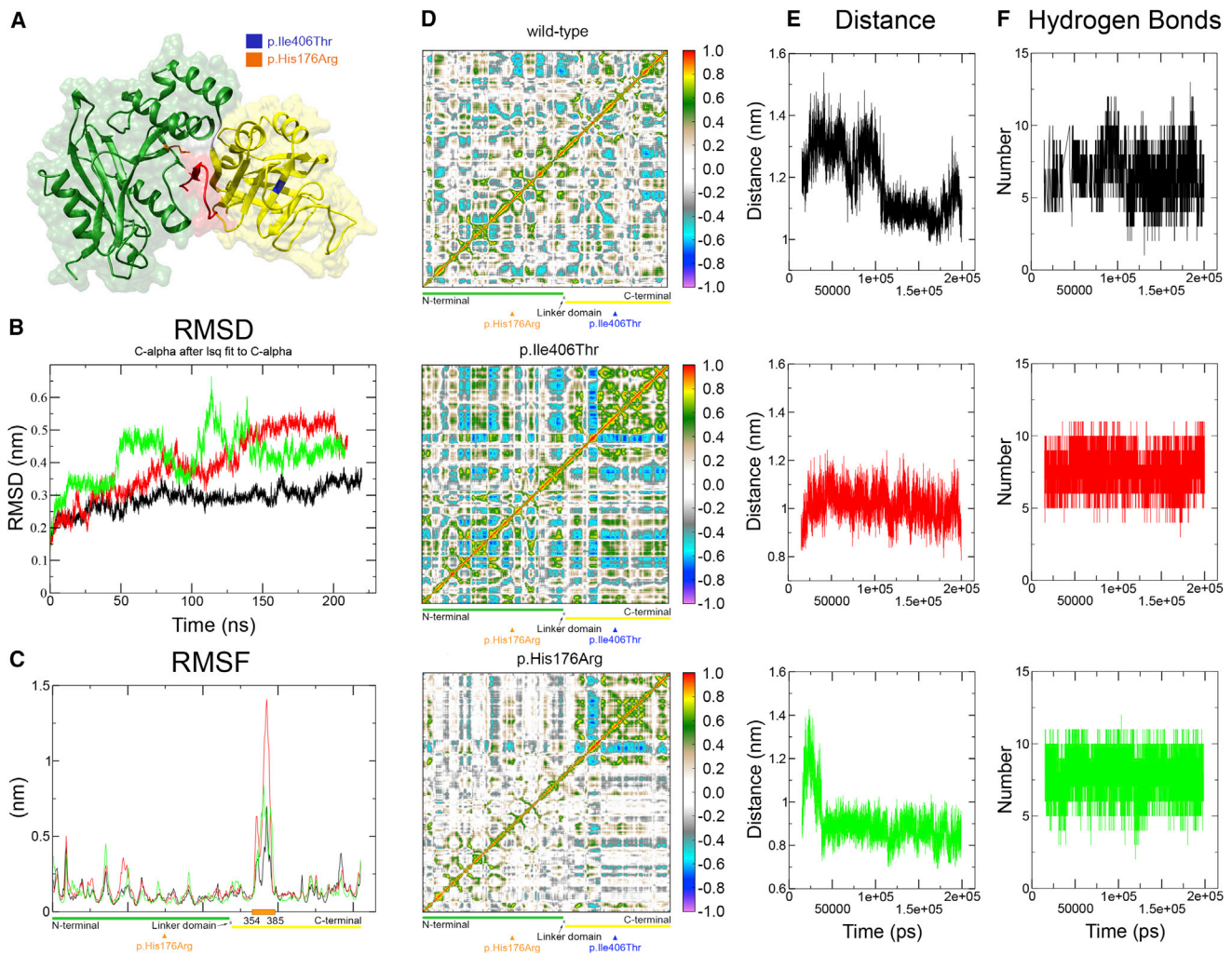
Figure 2. Analysis of MD Simulations of WT and Mutant SUFU Proteins

(A) 3D structure of SUFU-GLI complex. The N-terminal (28–262), C-terminal (266–285; 345–480), and linked (263–265) domains are colored green, yellow, and gray, respectively, while the GLI3 protein is colored in red. p.Ile406Thr is highlighted in blue and p.His176Arg in orange.

(B) RMSD of all heavy atoms of SUFU.

(C) RMSF of SUFU residues during simulations.

(D) Covariance matrix for SUFU WT (top), SUFU[p.Ile406Thr] (center), and SUFU[p.His176Arg] (bottom). Perfect direct or inverse correlations are highlighted in red or violet, respectively.

(E) Distances between amino acids forming the binding site for GLI3.

(F) H-bonds established during simulation between the residues forming the ligand binding pocket and GLI3.

In (B)–(F) graphs, SUFU WT is colored in black, SUFU[p.Ile406Thr] in red, and SUFU[p.His176Arg] in green.

subcellular localization of SUFU[p.Ile406Thr], which tended to form intracytoplasmic aggregates, while SUFU WT and SUFU[p.His176Arg] had uniform cytoplasmic and nuclear localization (Figure S4). Similar results were obtained in HeLa cells (data not shown).

SUFU protein levels are regulated within the cell mainly by degradation through the ubiquitin-proteasome system (UPS).[43] To test whether the observed reduction in SUFU levels was due to increased UPS-mediated degradation, transfected IMCD3 cells were treated with the proteasomal inhibitor MG132 for 6 hr and analyzed by WB. Proteasomal blockage induced the accumulation of both WT and mutant SUFU proteins, confirming that mutant proteins are processed through the UPS (Figure S5). To exclude

that the observed reduction of mutant SUFU was due to impaired protein synthesis, we treated control and mutant fibroblasts with cycloheximide, to block *de novo* synthesis of SUFU. Interestingly, the levels of both mutant SUFU proteins were slightly but significantly lower than controls even in basal conditions, and showed a more marked decrease after 24 hr treatment (Figure 3B). These findings support the observation that both missense variants increase the rate of SUFU degradation within cells.

SUFU Missense Variants Impair the Binding with GLI3 and Its Proteolytic Cleavage

Next, we focused on the interaction between SUFU and GLI3, since it is known that the major contribution to
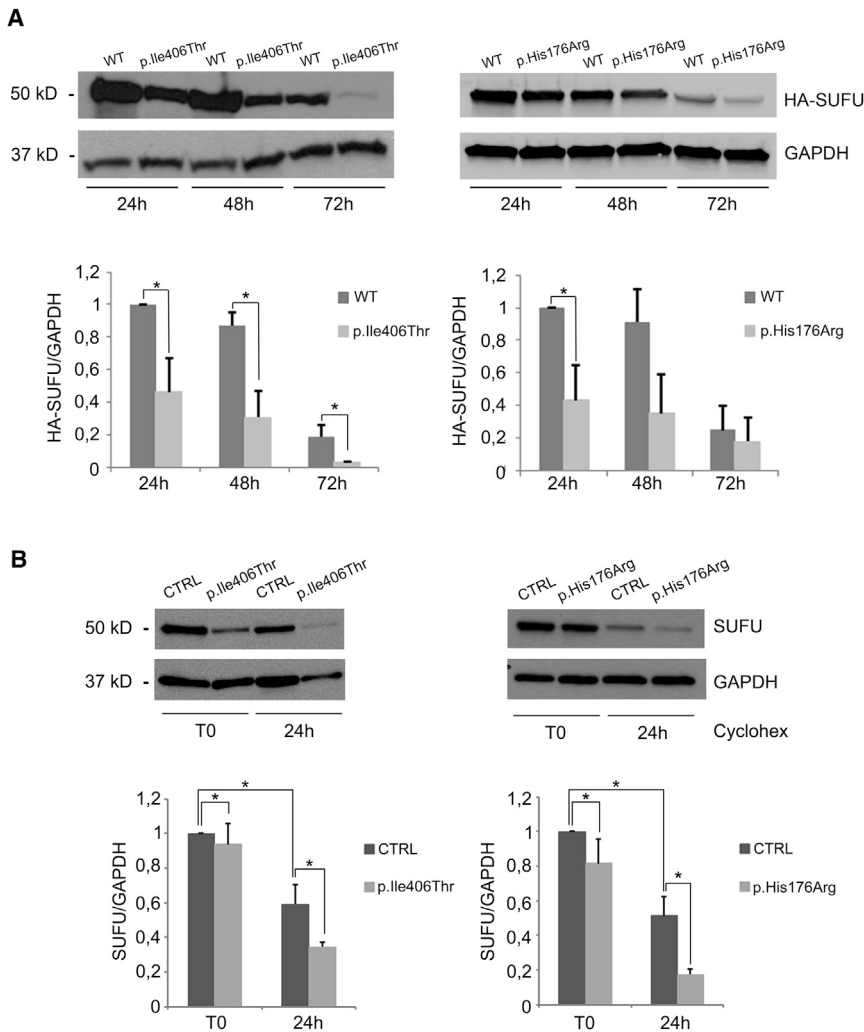
A

B

Figure 3. SUFU Missense Variants Reduce Protein Stability

(A) IMCD3 cells transfected with HA-tagged SUFU WT, SUFU$^{p.Ile406Thr}$, and SUFU$^{p.His176Arg}$ for 24, 48, and 72 hr show a more rapid decrease of mutant SUFU protein levels compared to WT (quantified by densitometry in the corresponding graphs).

(B) Control and mutant fibroblasts were treated with cycloheximide for 24 hr. Mutant cells show significantly lower levels of SUFU even in basal conditions, with a further more marked decrease after treatment.

Results are representative of at least three independent experiments. Graphs represent means ± standard errors. *p < 0.05.

the repressor forms of GLI comes from GLI3. Indeed, cleaved GLI3R suppresses SHH target genes when the pathway is inactive, while activated GLI2 triggers target gene expression upon stimulation of the pathway.[15]

To examine whether the identified missense variants could affect SUFU-GLI3 binding, as suggested by MD simulations, co-immunoprecipitation experiments were performed on total protein extracts of IMCD3 cells transfected with either HA-tagged SUFU WT, SUFU$^{p.Ile406Thr}$, or SUFU$^{p.His176Arg}$. The binding of unprocessed GLI3 was significantly higher with SUFU WT than with either of the two mutant proteins, suggesting that both missense variants impaired the ability of SUFU to bind GLI3 (Figure 4A). To further confirm this finding, we measured by WB analysis the levels of GLI3 full length and GLI3R in control or mutant fibroblasts cultured in the presence or absence of SAG, a SMO agonist able to activate the SHH pathway. As expected, in control fibroblasts, both GLI3 full length and GLI3R levels decreased after SAG treatment.[44] In mutant cells, GLI3 full length and GLI3R levels were already significantly lower than control in untreated conditions, with a further slight decrease

upon SAG stimulation (Figures 4B and S6). Taken together, these results suggest that the identified missense variants reduce the binding affinity of SUFU to GLI3, resulting in impaired repression of the pathway in basal conditions.

To test whether mutant SUFU proteins also showed impaired binding to GLI1, an effector of the pathway lacking repressor properties,[41] we performed immunofluorescence and co-immunoprecipitation experiments in IMCD3 cells co-transfected with plasmids expressing either WT or mutant SUFU and GLI1. However, we did not observe any notable difference in co-localization of the two proteins, nor in SUFU-GLI1 binding (Figure S7).
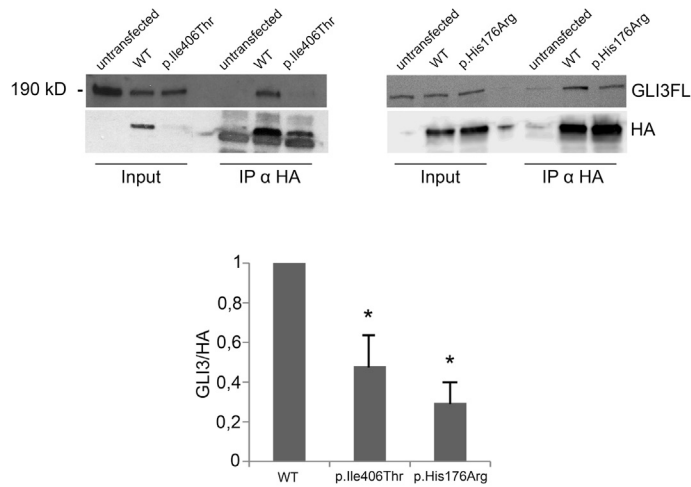
SUFU Missense Variants Impair Repression of the SHH Pathway

In light of the previous results, we sought to assess whether the SHH pathway was deregulated in the presence of mutant SUFU. To this aim, we evaluated by quantitative real-time PCR in control and mutant fibroblasts the expression levels of 14 genes, including several target genes of the SHH pathway and representative genes of other developmental pathways such as BMP, canonical Wnt, and non-canonical Wnt/planar cell polarity (PCP) pathways.

Interestingly, the basal expression levels of the key SHH-target genes BCL2, GLI1, and PTCH1 were significantly higher in both mutant fibroblasts compared to control, with a limited further increase upon SAG stimulation. Conversely, mutant cells showed markedly lower basal expression levels of VANGL2 (involved in the PCP pathway), which were only minimally perturbed after SAG treatment (Figure 5). These altered expression levels could be partially rescued by overexpression of SUFU WT in mutant fibroblasts (data not shown). Other genes
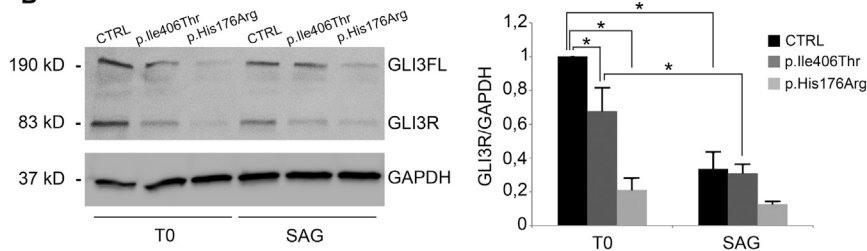
A

B

appeared to be deregulated without reaching statistical significance, or remained unperturbed (Table S4). These findings confirm the previous observations that the identified missense variants impair the ability of SUFU to constitutively repress the SHH pathway, which results in deregulation of target gene expression especially in unstimulated conditions.

Discussion

Here we report the occurrence of homozygous missense variants in *SUFU* in four children from two consanguineous, unrelated families presenting with mild features of JS associated with peculiar cranio-facial anomalies and polydactyly. Functional studies on fibroblasts and cell lines showed that the mutant proteins were less stable and more rapidly degraded than SUFU WT and had impaired ability to bind GLI3 and promote its cleavage into the repressor form GLI3R, while they maintained unaltered ability to bind GLI1. These findings suggest that both variants are hypomorphic alleles, resulting only in a partial loss of the normal gene function. This is in line with the previous observations that complete *Sufu* knock-out is lethal in mouse embryos[31] and that human *SUFU* is extremely intolerant to loss of function and generally intolerant to variation. In fact, homozygous loss-of-function variants were never observed in more than 138,000 individuals from the gnomAD database (pLI score = 1),[45] and even synonymous and missense variants

were observed at significantly lower frequency than expected (positive Z scores of 1.82 and 2.54, respectively) and nearly always in the heterozygous state. Of note, the Geno2MP database reports the occurrence of a rare, potentially harmful homozygous missense variant in *SUFU* (p.Ala425Val, CADD score 18.38) in a single subject with reported cerebellar anomalies. Although we were not able to get in touch with the referring clinician, this individual may represent yet another case of *SUFU* recessive hypomorphic mutations giving rise to a neurodevelopmental phenotype.

We also identified heterozygous rare variants of *SUFU* in 12 children with JS, none of which had developed any tumors or signs of Gorlin syndrome. Eight variants were missense changes largely predicted as benign, and in fact biallelic pathogenic mutations in a well-established JS-associated gene were detected in five carriers (Table S3). The other four *SUFU* variants included a splice site variant and three loss-of-function variants predicted to result in *SUFU* haploinsufficiency. Three variants had been inherited by a healthy parent, while one appeared to have arisen *de novo*. Interestingly, the frequency of *SUFU* heterozygous loss-of-function variants among JS-affected subjects (3/761) is markedly higher than the frequency reported in gnomAD database (4/138,629, p < 2^{-16}), suggesting a potential role of SUFU haploinsufficiency in the determination of the JS phenotype. On the other hand, *SUFU* heterozygous loss-of-function variants have been described in several young children diagnosed with medulloblastoma, often inherited from a healthy parent.[27] While macrocephaly and/or hypertelorism have been reported in a subset of these case subjects, we could not find any mention of developmental delay, ataxia, or intellectual impairment, nor of the presence of congenital cerebellar or brainstem malformations that would suggest a diagnosis of JS in any of these published case subjects. Thus, at present, the significance of SUFU heterozygous variants in the context of JS remains to be determined.
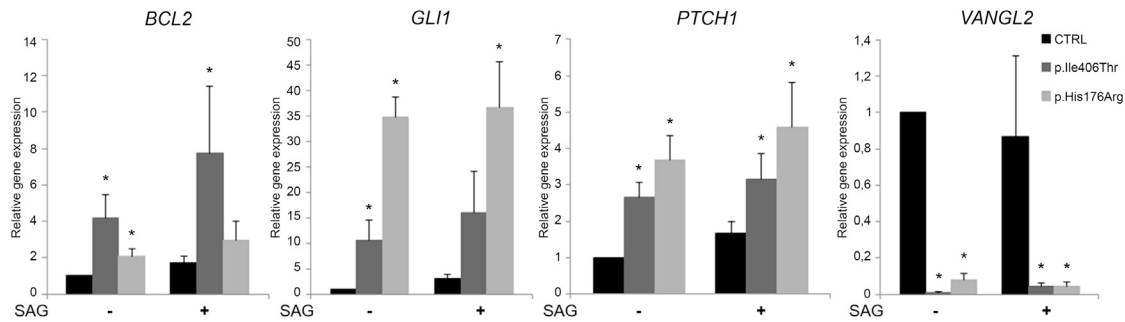
Figure 5.   The SHH Pathway Is Deregulated in Mutant Fibroblasts
Histograms show the expression levels of four target genes that in basal conditions are either significantly overexpressed (*BCL2*, *GLI1*, and *PTCH1*) or under-expressed (*VANGL2*) in fibroblasts from the two probands compared to control subjects. Results are representative of three independent experiments. Graphs represent means ± standard errors. *p < 0.05.

Recently, Makino and collaborators generated *Sufu* knock-in mice homozygous for the missense variant p.Thr396Ile, which lies only ten amino acids away from the homozygous variant p.Ile406Thr identified in family COR369. These animals died later than knock-out mice (at E14–E18) and showed a spectrum of developmental anomalies including cranio-facial defects and polydactyly, which were similar to those observed in mice lacking *Gli3*, but not in those lacking *Gli1* or *Gli2*. In line with this, a functional characterization of Sufu[T396I/T396I] mice showed reduced stability of mutant Sufu and significantly reduced levels of Gli3 full length and Gli3R, without quantitatively affecting the levels of either Gli1 or Gli2.[46] Intriguingly, the clinical and functional anomalies of this *knock-in* model closely resemble those of the affected children described here and support our observation that recessive hypomorphic variants in *SUFU* may induce deregulation of the SHH pathway through two distinct mechanisms: on one hand by reducing SUFU half-life within cells, on the other hand by selectively impairing its interaction with GLI3 and the subsequent formation of GLI3R.

In line with these observations and with the notion that GLI3R is the principal repressor of SHH signaling,[15] we found in basal conditions a significant overexpression of three key target genes (namely *BCL2*, *GLI1*, and *PTCH1*) in mutant fibroblasts compared to controls. Upon SAG-induced activation of the SHH pathway, which is mainly mediated by GLI1 and GLI2A, the expression levels of these genes further increased, as expected. Interestingly, in both mutant fibroblasts we also observed a marked downregulation of the expression levels of *VANGL2*, a gene encoding for a protein of the non-canonical Wnt/PCP pathway, which also requires primary cilia for its activation.[47] In particular, VANGL2 has been implicated in neuronal migration and post-crossing commissural axonal guidance;[48,49] our observations in mutant fibroblasts suggest that SUFU might play an important role in sustaining *VANGL2* expression levels and that alterations of the PCP pathway may contribute to the developmental defects in individuals carrying *SUFU* hypomorphic variants.

Further support to the link between the identified *SUFU* variants and a deregulation of SHH signaling comes from

the observed phenotype, which is mainly characterized by (1) typical cranio-facial dysmorphisms (hypertelorism, depressed nasal bridge, frontal bossing, macrocephaly); (2) developmental delay, mild intellectual impairment, ataxia, and ocular-motor apraxia; (3) cerebellar vermis hypoplasia with dysplastic foliar pattern and mildly elongated superior cerebellar peduncles (mild MTS); and (4) postaxial polydactyly. This clinical presentation shares features both with ciliopathies such as JS and with syndromes characterized by impaired repression of the SHH pathway.

JS is typically diagnosed by the presence of the MTS, and more than 30 genes associated to JS have been identified to date.[50] Among these, recessive pathogenic variants in *KIF7* were found to cause a spectrum of anomalies ranging from pure JS to ACLS, which is characterized by the MTS, corpus callosum agenesis, pre- and post-axial polydactyly, and similar cranio-facial abnormalities as shown by *SUFU*-mutated individuals. Interestingly, *KIF7* is a ciliary protein that promotes the localization and appropriate regulation of SUFU and GLI proteins at the ciliary tip.[19,51] In the absence of functional KIF7, the ciliary tip compartment becomes disorganized, leading to the formation of ectopic tip-like compartments where GLI-SUFU complexes localize and are inappropriately activated even in the absence of SHH ligand.[52]

The same constellation of cranio-facial abnormalities along with developmental delay and polysyndactyly is detected in GCPS, in which heterozygous *GLI3* variants result in reduced levels of Gli3R.[21] Recently, a recurrent mosaic heterozygous nonsynonymous variant in *SMO* (c.1234C>T [p.Leu412Phe]) causing overactivation of the SHH pathway was found to cause CJS, a multisystem disorder characterized by patchy skin lesions, unicoronal craniosynostosis, iris colobomas, microphthalmia, and intestinal malrotation. Of note, subjects with CJS also present similar cranio-facial dysmorphisms and polysyndactyly, as well as a spectrum of cerebral malformations including mild cerebellar hypoplasia, corpus callosum abnormalities, and polymicrogyria.[23]

Moreover, a proportion of subjects with Gorlin syndrome, caused by heterozygous loss-of-function variants of either *PTCH1* or *SUFU*, variably exhibit macrocephaly,

hypertelorism, depressed nasal bridge, post-axial polydactyly, as well as macrosomia and dyskeratotic plantar pits (present in family COR369).[24] These observations suggest that these peculiar cranio-facial and digit anomalies are strictly related to abnormal activation of the SHH pathway, caused either by reduced levels (or functioning) of repressor proteins or by the constitutive activation of proteins that transduce SHH signaling. Conversely, genetic changes impairing activation of the SHH pathway, such as heterozygous variants of *SHH* or *GLI2*, are consistently associated with opposite cranio-facial dysmorphisms such as microcephaly, hypotelorism, microphthalmia, midface hypoplasia, and cleft lip/palate, that variably associate with forebrain cleavage anomalies (defining the holoprosencephaly spectrum) and digital number abnormalities.[15,20]

None of the other features typical of Gorlin syndrome (keratocystic odontogenic tumors, ribs and spine abnormalities, calcification of the falx cerebri) were present in the four children carrying recessive *SUFU* variants, nor had they developed any cancer. This could be related to the fact that these clinical features may only manifest in the presence of SUFU haploinsufficiency (and often in conjunction with a somatic "second hit" in cancer cells), while SUFU proteins carrying hypomorphic variants were defective in only selected properties. However, all children are still young, and a longer follow-up will be needed to definitely exclude the occurrence of tumors.

The observed phenotypic variability observed in carriers of *SUFU*-recessive variants is not surprising, as it is also observed in most ciliopathies as well as in other defects of the SHH pathway.[20,22] In particular, the observed different impact of the two missense variants on SUFU subcellular distribution and degradation, GLI3 cleavage, and expression of target genes may enlighten some differences between the two families, such as the occurrence, in family COR369, of more severe polydactyly and of asymmetric polymicrogyria, prevalent in the perisylvian regions.

Polymicrogyria has been occasionally reported in subjects with JS caused by pathogenic variants in distinct ciliary genes,[18,53,54] as well as in a boy with schizencephaly and partial absence of the corpus callosum carrying a *SHH* heterozygous variant.[55] Moreover, two families with isolated diffuse polymicrogyria were found to carry recessive pathogenic variants in *RTTN* encoding Rotatin, a centrosome-associated protein essential for maintaining normal ciliary structure and functioning. Interestingly, an expression study in *RTTN* mutant fibroblasts showed a significant deregulation of several genes involved in the SHH and WNT pathways, similarly to what we observed in *SUFU* mutant cells.[56] Taken together, these observations support the finding that polymicrogyria can be part of the spectrum of brain developmental anomalies associated with deregulation of SHH signaling.

Besides *SUFU* p.Ile406Thr, the two affected siblings in family COR369 also shared the homozygous variant p.Thr716Ser in *CDHR1*. Pathogenic variants of this gene are known to cause an autosomal-recessive form of cone-rod dystrophy with onset in the late second decade of life, thus at a later age than that of both siblings, who had preserved visual acuity and normal fundoscopy. However, it is worth noting that an electroretinogram performed in the brother showed signs of underlying retinopathy, requiring further investigation and follow-up.

In conclusion, we report that germline recessive hypomorphic variants in *SUFU* may alter its stability and function as repressor of the SHH pathway, giving rise to a peculiar spectrum of developmental defects sharing features of ciliopathies such as JS and of SHH-related disorders. The occurrence of specific cranio-facial and digit abnormalities should represent red flags implicating an underlying defect of genes involved in the SHH pathway.

Accession Numbers

The accession numbers for the SUFU variants reported in this article are LOVD: 0000104436, 0000104437, 0000104738, and 0000104739. See Table S2.

Supplemental Data

Supplemental Data include a Supplemental Note, seven figures, four tables, and one movie and can be found with this article online at http://dx.doi.org/10.1016/j.ajhg.2017.08.017.

Web Resources

dbSNP, https://www.ncbi.nlm.nih.gov/projects/SNP/
Geno2MP, http://geno2mp.gs.washington.edu/Geno2MP/#/
gnomAD Browser, http://gnomad.broadinstitute.org/
Human Longevity Database, https://search.hli.io/?q=
LOVD, http://www.lovd.nl/3.0/home
NHLBI Exome Sequencing Project (ESP) Exome Variant Server, http://evs.gs.washington.edu/EVS/
OMIM, http://www.omim.org/
R statistical software, http://www.r-project.org/

References

1. Gorojankina, T. (2016). Hedgehog signaling pathway: a novel model and molecular mechanisms of signal transduction. Cell. Mol. Life Sci. *73*, 1317–1332.

2. Gupta, S., and Sen, J. (2016). Roof plate mediated morphogenesis of the forebrain: New players join the game. Dev. Biol. *413*, 145–152.

3. Wechsler-Reya, R.J., and Scott, M.P. (1999). Control of neuronal precursor proliferation in the cerebellum by Sonic Hedgehog. Neuron *22*, 103–114.

4. De Luca, A., Cerrato, V., Fucà, E., Parmigiani, E., Buffo, A., and Leto, K. (2016). Sonic hedgehog patterning during cerebellar development. Cell. Mol. Life Sci. *73*, 291–303.

5. Lopez-Rios, J. (2016). The many lives of SHH in limb development and evolution. Semin. Cell Dev. Biol. *49*, 116–124.

6. Tukachinsky, H., Lopez, L.V., and Salic, A. (2010). A mechanism for vertebrate Hedgehog signaling: recruitment to cilia and dissociation of SuFu-Gli protein complexes. J. Cell Biol. *191*, 415–428.

7. Ruat, M., Roudaut, H., Ferent, J., and Traiffort, E. (2012). Hedgehog trafficking, cilia and brain functions. Differentiation *83*, S97–S104.

8. Han, Y.G., Spassky, N., Romaguera-Ros, M., Garcia-Verdugo, J.M., Aguilar, A., Schneider-Maunoury, S., and Alvarez-Buylla, A. (2008). Hedgehog signaling and primary cilia are required for the formation of adult neural stem cells. Nat. Neurosci. *11*, 277–284.

9. Spassky, N., Han, Y.G., Aguilar, A., Strehl, L., Besse, L., Laclef, C., Ros, M.R., Garcia-Verdugo, J.M., and Alvarez-Buylla, A. (2008). Primary cilia are required for cerebellar development and Shh-dependent expansion of progenitor pool. Dev. Biol. *317*, 246–259.

10. Aguilar, A., Meunier, A., Strehl, L., Martinovic, J., Bonniere, M., Attie-Bitach, T., Encha-Razavi, F., and Spassky, N. (2012). Analysis of human samples reveals impaired SHH-dependent cerebellar development in Joubert syndrome/ Meckel syndrome. Proc. Natl. Acad. Sci. USA *109*, 16951–16956.

11. Larkins, C.E., Aviles, G.D., East, M.P., Kahn, R.A., and Caspary, T. (2011). Arl13b regulates ciliogenesis and the dynamic localization of Shh signaling proteins. Mol. Biol. Cell *22*, 4694–4703.

12. Briscoe, J., and Thérond, P.P. (2013). The mechanisms of Hedgehog signalling and its roles in development and disease. Nat. Rev. Mol. Cell Biol. *14*, 416–429.

13. Nozawa, Y.I., Lin, C., and Chuang, P.T. (2013). Hedgehog signaling from the primary cilium to the nucleus: an emerging picture of ciliary localization, trafficking and transduction. Curr. Opin. Genet. Dev. *23*, 429–437.

14. Katoh, Y., and Katoh, M. (2009). Hedgehog target genes: mechanisms of carcinogenesis induced by aberrant hedgehog signaling activation. Curr. Mol. Med. *9*, 873–886.

15. Hui, C.C., and Angers, S. (2011). Gli proteins in development and disease. Annu. Rev. Cell Dev. Biol. *27*, 513–537.

16. Romani, M., Micalizzi, A., and Valente, E.M. (2013). Joubert syndrome: congenital cerebellar ataxia with the molar tooth. Lancet Neurol. *12*, 894–905.

17. Poretti, A., Vitiello, G., Hennekam, R.C., Arrigoni, F., Bertini, E., Borgatti, R., Brancati, F., D'Arrigo, S., Faravelli, F., Giordano, L., et al. (2012). Delineation and diagnostic criteria of Oral-Facial-Digital Syndrome type VI. Orphanet J. Rare Dis. *7*, 4.

18. Dixon-Salazar, T., Silhavy, J.L., Marsh, S.E., Louie, C.M., Scott, L.C., Gururaj, A., Al-Gazali, L., Al-Tawari, A.A., Kayserili, H., Sztriha, L., and Gleeson, J.G. (2004). Mutations in the AHI1 gene, encoding jouberin, cause Joubert syndrome with cortical polymicrogyria. Am. J. Hum. Genet. *75*, 979–987.

19. Putoux, A., Thomas, S., Coene, K.L., Davis, E.E., Alanay, Y., Ogur, G., Uz, E., Buzas, D., Gomes, C., Patrier, S., et al. (2011). KIF7 mutations cause fetal hydrolethalus and acrocallosal syndromes. Nat. Genet. *43*, 601–606.

20. Dubourg, C., Carré, W., Hamdi-Rozé, H., Mouden, C., Roume, J., Abdelmajid, B., Amram, D., Baumann, C., Chassaing, N., Coubes, C., et al. (2016). Mutational spectrum in holoprosencephaly shows that FGF is a new major signaling pathway. Hum. Mutat. *37*, 1329–1339.

21. Johnston, J.J., Olivos-Glander, I., Killoran, C., Elson, E., Turner, J.T., Peters, K.F., Abbott, M.H., Aughton, D.J., Aylsworth, A.S., Bamshad, M.J., et al. (2005). Molecular and clinical analyses of Greig cephalopolysyndactyly and Pallister-Hall syndromes: robust phenotype prediction from the type and position of GLI3 mutations. Am. J. Hum. Genet. *76*, 609–622.

22. Démurger, F., Ichkou, A., Mougou-Zerelli, S., Le Merrer, M., Goudefroye, G., Delezoide, A.L., Quélin, C., Manouvrier, S., Baujat, G., Fradin, M., et al. (2015). New insights into genotype-phenotype correlation for GLI3 mutations. Eur. J. Hum. Genet. *23*, 92–102.

23. Twigg, S.R.F., Hufnagel, R.B., Miller, K.A., Zhou, Y., McGowan, S.J., Taylor, J., Craft, J., Taylor, J.C., Santoro, S.L., Huang, T., et al. (2016). A recurrent mosaic mutation in SMO, encoding the Hedgehog signal transducer Smoothened, is the major cause of Curry-Jones syndrome. Am. J. Hum. Genet. *98*, 1256–1265.

24. Kiwilsza, M., and Sporniak-Tutak, K. (2012). Gorlin-Goltz syndrome–a medical condition requiring a multidisciplinary approach. Med. Sci. Monit. *18*, RA145–RA153.

25. Pastorino, L., Ghiorzo, P., Nasti, S., Battistuzzi, L., Cusano, R., Marzocchi, C., Garrè, M.L., Clementi, M., and Scarrà, G.B. (2009). Identification of a SUFU germline mutation in a family with Gorlin syndrome. Am. J. Med. Genet. A. *149A*, 1539–1543.

26. Brugières, L., Pierron, G., Chompret, A., Paillerets, B.B., Di Rocco, F., Varlet, P., Pierre-Kahn, A., Caron, O., Grill, J., and Delattre, O. (2010). Incomplete penetrance of the predisposition to medulloblastoma associated with germ-line SUFU mutations. J. Med. Genet. *47*, 142–144.

27. Brugières, L., Remenieras, A., Pierron, G., Varlet, P., Forget, S., Byrde, V., Bombled, J., Puget, S., Caron, O., Dufour, C., et al. (2012). High frequency of germline SUFU mutations in children with desmoplastic/nodular medulloblastoma younger than 3 years of age. J. Clin. Oncol. *30*, 2087–2093.

28. Aavikko, M., Li, S.P., Saarinen, S., Alhopuro, P., Kaasinen, E., Morgunova, E., Li, Y., Vesanen, K., Smith, M.J., Evans, D.G., et al. (2012). Loss of SUFU function in familial multiple meningioma. Am. J. Hum. Genet. *91*, 520–526.

29. Taylor, M.D., Liu, L., Raffel, C., Hui, C.C., Mainprize, T.G., Zhang, X., Agatep, R., Chiappa, S., Gao, L., Lowrance, A., et al. (2002). Mutations in SUFU predispose to medulloblastoma. Nat. Genet. *31*, 306–310.

30. Teglund, S., and Toftgård, R. (2010). Hedgehog beyond medulloblastoma and basal cell carcinoma. Biochim. Biophys. Acta *1805*, 181–208.

31. Svärd, J., Heby-Henricson, K., Persson-Lek, M., Rozell, B., Lauth, M., Bergström, A., Ericson, J., Toftgård, R., and Teglund, S. (2006). Genetic elimination of Suppressor of fused reveals an essential repressor function in the mammalian Hedgehog signaling pathway. Dev. Cell 10, 187–197.

32. Goodrich, L.V., Milenković, L., Higgins, K.M., and Scott, M.P. (1997). Altered neural cell fates and medulloblastoma in mouse patched mutants. Science 277, 1109–1113.

33. Zhulyn, O., and Hui, C.C. (2015). Sufu and Kif7 in limb patterning and development. Dev. Dyn. 244, 468–478.

34. Zhulyn, O., Li, D., Deimling, S., Vakili, N.A., Mo, R., Puviindran, V., Chen, M.H., Chuang, P.T., Hopyan, S., and Hui, C.C. (2014). A switch from low to high Shh activity regulates establishment of limb progenitors and signaling centers. Dev. Cell 29, 241–249.

35. Kim, J.J., Gill, P.S., Rotin, L., van Eede, M., Henkelman, R.M., Hui, C.C., and Rosenblum, N.D. (2011). Suppressor of fused controls mid-hindbrain patterning and cerebellar morphogenesis via GLI3 repressor. J. Neurosci. 31, 1825–1836.

36. Roosing, S., Romani, M., Isrie, M., Rosti, R.O., Micalizzi, A., Musaev, D., Mazza, T., Al-Gazali, L., Altunoglu, U., Boltshauser, E., et al. (2016). Mutations in CEP120 cause Joubert syndrome as well as complex ciliopathy phenotypes. J. Med. Genet. 53, 608–615.

37. Romani, M., Mehawej, C., Mazza, T., Mégarbané, A., and Valente, E.M. (2016). "Fork and bracket" syndrome expands the spectrum of SBF1-related sensory motor polyneuropathies. Neurol Genet 2, e61.

38. Cherry, A.L., Finta, C., Karlström, M., Jin, Q., Schwend, T., Astorga-Wells, J., Zubarev, R.A., Del Campo, M., Criswell, A.R., de Sanctis, D., et al. (2013). Structural basis of SUFU-GLI interaction in human Hedgehog signalling regulation. Acta Crystallogr. D Biol. Crystallogr. 69, 2563–2579.

39. Pettersen, E.F., Goddard, T.D., Huang, C.C., Couch, G.S., Greenblatt, D.M., Meng, E.C., and Ferrin, T.E. (2004). UCSF Chimera–a visualization system for exploratory research and analysis. J. Comput. Chem. 25, 1605–1612.

40. D'Amico, D., Antonucci, L., Di Magno, L., Coni, S., Sdruscia, G., Macone, A., Miele, E., Infante, P., Di Marcotullio, L., De Smaele, E., et al. (2015). Non-canonical Hedgehog/AMPK-mediated control of polyamine metabolism supports neuronal and medulloblastoma cell growth. Dev. Cell 35, 21–35.

41. Dunaeva, M., Michelson, P., Kogerman, P., and Toftgard, R. (2003). Characterization of the physical interaction of Gli proteins with SUFU proteins. J. Biol. Chem. 278, 5116–5122.

42. Dafinger, C., Liebau, M.C., Elsayed, S.M., Hellenbroich, Y., Boltshauser, E., Korenke, G.C., Fabretti, F., Janecke, A.R., Ebermann, I., Nürnberg, G., et al. (2011). Mutations in KIF7 link Joubert syndrome with Sonic Hedgehog signaling and microtubule dynamics. J. Clin. Invest. 121, 2662–2667.

43. Yue, S., Chen, Y., and Cheng, S.Y. (2009). Hedgehog signaling promotes the degradation of tumor suppressor Sufu through the ubiquitin-proteasome pathway. Oncogene 28, 492–499.

44. Humke, E.W., Dorn, K.V., Milenkovic, L., Scott, M.P., and Rohatgi, R. (2010). The output of Hedgehog signaling is controlled by the dynamic association between Suppressor of Fused and the Gli proteins. Genes Dev. 24, 670–682.

45. Lek, M., Karczewski, K.J., Minikel, E.V., Samocha, K.E., Banks, E., Fennell, T., O'Donnell-Luria, A.H., Ware, J.S., Hill, A.J., Cummings, B.B., et al.; Exome Aggregation Consortium (2016). Analysis of protein-coding genetic variation in 60,706 humans. Nature 536, 285–291.

46. Makino, S., Zhulyn, O., Mo, R., Puviindran, V., Zhang, X., Murata, T., Fukumura, R., Ishitsuka, Y., Kotaki, H., Matsumaru, D., et al. (2015). T396I mutation of mouse Sufu reduces the stability and activity of Gli3 repressor. PLoS ONE 10, e0119455.

47. Wallingford, J.B., and Mitchell, B. (2011). Strange as it may seem: the many links between Wnt signaling, planar cell polarity, and cilia. Genes Dev. 25, 201–213.

48. Shafer, B., Onishi, K., Lo, C., Colakoglu, G., and Zou, Y. (2011). Vangl2 promotes Wnt/planar cell polarity-like signaling by antagonizing Dvl1-mediated feedback inhibition in growth cone guidance. Dev. Cell 20, 177–191.

49. Tissir, F., and Goffinet, A.M. (2013). Shaping the nervous system: role of the core planar cell polarity genes. Nat. Rev. Neurosci. 14, 525–535.

50. Mitchison, H.M., and Valente, E.M. (2017). Motile and non-motile cilia in human pathology: from function to phenotypes. J. Pathol. 241, 294–309.

51. Putoux, A., Nampoothiri, S., Laurent, N., Cormier-Daire, V., Beales, P.L., Schinzel, A., Bartholdi, D., Alby, C., Thomas, S., El-khartoufi, N., et al. (2012). Novel KIF7 mutations extend the phenotypic spectrum of acrocallosal syndrome. J. Med. Genet. 49, 713–720.

52. He, M., Subramanian, R., Bangs, F., Omelchenko, T., Liem, K.F., Jr., Kapoor, T.M., and Anderson, K.V. (2014). The kinesin-4 protein Kif7 regulates mammalian Hedgehog signalling by organizing the cilium tip compartment. Nat. Cell Biol. 16, 663–672.

53. Giordano, L., Vignoli, A., Pinelli, L., Brancati, F., Accorsi, P., Faravelli, F., Gasparotti, R., Granata, T., Giaccone, G., Inverardi, F., et al. (2009). Joubert syndrome with bilateral polymicrogyria: clinical and neuropathological findings in two brothers. Am. J. Med. Genet. A. 149A, 1511–1515.

54. Field, M., Scheffer, I.E., Gill, D., Wilson, M., Christie, L., Shaw, M., Gardner, A., Glubb, G., Hobson, L., Corbett, M., et al. (2012). Expanding the molecular basis and phenotypic spectrum of X-linked Joubert syndrome associated with OFD1 mutations. Eur. J. Hum. Genet. 20, 806–809.

55. Schell-Apacik, C.C., Ertl-Wagner, B., Panzel, A., Klausener, K., Rausch, G., Muenke, M., von Voss, H., and Hehr, U. (2009). Maternally inherited heterozygous sequence change in the sonic hedgehog gene in a male patient with bilateral closed-lip schizencephaly and partial absence of the corpus callosum. Am. J. Med. Genet. A. 149A, 1592–1594.

56. Kheradmand Kia, S., Verbeek, E., Engelen, E., Schot, R., Poot, R.A., de Coo, I.F., Lequin, M.H., Poulton, C.J., Pourfarzad, F., Grosveld, F.G., et al. (2012). RTTN mutations link primary cilia function to organization of the human cerebral cortex. Am. J. Hum. Genet. 91, 533–540.